30

Composite Cathode Material for Li-Ion Batteries Based on $LiFePO_4$ System

Janina Molenda[1] and Marcin Molenda[2]
[1]*AGH University of Science and Technology*
Faculty of Energy and Fuels, Krakow
[2]*Jagiellonian University, Faculty of Chemistry,Krakow*
Poland

1. Introduction

Huge development electric vehicles market and storage energy in renewable energy systems forces usage of batteries characterized by high volumetric and gravimetric density of stored energy, exhibiting large number of charge/discharge cycles, being safe for user as well as of low environmental impact and low cost. The widespread technology of reversible Ni-Cd and NiMH cells reached the theoretical limit of available improvements. Promising for the future and still undergoing rapid development is the technology of reversible lithium cells, commonly known as *Li-ion batteries*. The required capacity of a Li-ion battery for vehicle applications and renewable energy systems is much bigger than for portable electronics – 20-100 kWh. The security of usage of that kind of batteries is an important issue. The bigger the capacity, the more energy is accumulated – therefore, more strict security measures must apply. This raises numerous challenges to develop new material technologies – cell components with a better chemical and thermal stability, as well as to solve problems such as heat dissipation dependent on the cell housing system. The lack of experimental data on real lifetimes of Li-ion batteries in changeable climatic conditions – from +40°C to -40°C (the required lifetime of batteries is ten years for vehicles and 1-4 years for laptops) constitutes also a big problem.

2. How does a Li-ion battery function and how can it be improved?

Li-ion batteries are based on capability of transition metals compounds M_aX_b (M- transition metal; X = O, S) with layered or tunnel structure to reversibly insert lithium (one or more mol Li per mol M_aX_b) at room temperature without significant changes in their crystallographic structure (*intercalation process*) (Whittingham, 1978; Tarascon & Armand, 2001; Ohzuku, 1993). Fig.1 presents different type structures capable to intercalation process. In this process, the basic elements of the structure do not undergo any changes, except for minor reversible variations of lattice parameters. Stability of structure during the whole process is due to strong ionic and covalent bonds between M and X atoms.
The intercalation of lithium (which is always a combined ionic- electronic transport process, involving insertion of Li^+ ions and an equivalent number of electrons) to transition metal compounds M_aX_b can be put down as follows:

$$xLi^+ + x\,e^- + M_aX_b = Li_xM_aX_b \quad (1)$$

This reaction makes use of deep *d-type* energy levels in transition metal compounds, with the energy of several eV/atom, which can accumulate the energy of several kWh/kg; thus enabling construction of a power supply with significant volumetric and gravimetric energy density.

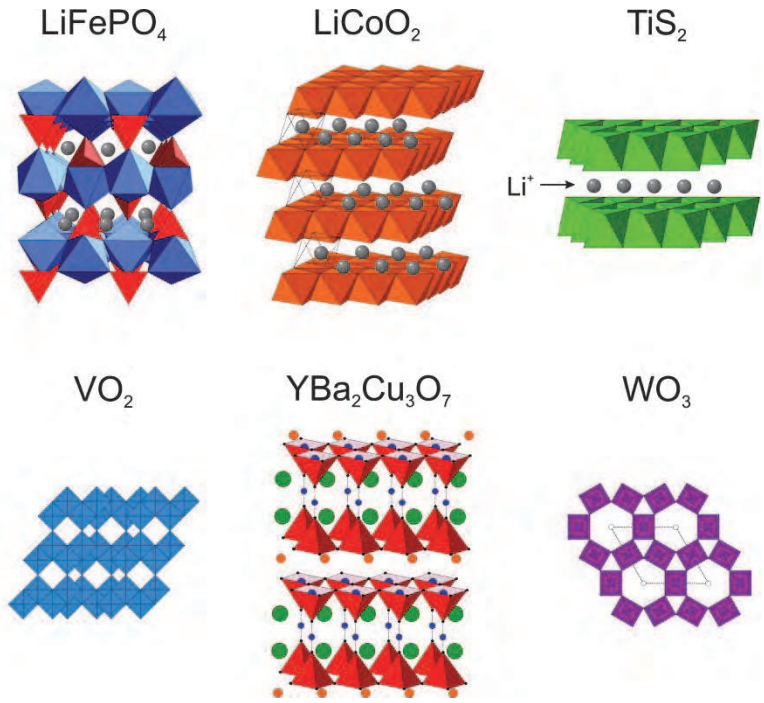

Fig. 1. Different type structures capable to lithium intercalation.

Numerous works on cathode materials by J. Molenda: Li_xTiS_2 (Than et al., 1991), Li_xVO_2 (J. Molenda & Kubik, 1993), Li_xCoO_2 (J. Molenda & Stokłosa, 1989), Li_xNiO_2 (J. Molenda et al., 2002), Li_xWO_3 (J. Molenda & Kubik, 1989), $Li_xYBa_2Cu_3O_7$ (J. Molenda et al., 1993), $Li_xMn_2O_4$ (J. Molenda et al., 2000; J. Molenda et al., 2004), Li–graphite (J. Molenda, 1997), Li_xFePO_4 (J. Molenda et al., 2006) prove the key role of electronic structure on the intercalation process. Variations of the EMF of the $Li/Li^+/Li_xM_aX_b$ cell corresponds to those of electrochemical potential of electrons (Fermi level) of the cathode material brought about by lithium intercalation (J. Molenda et al., 2005). The electrons introduced during intercalation process (with equivalent number of Li^+ ions) take available electronic levels and rise the position of the Fermi level in a way dependant of the density of states function (DOS). A high density of states at the Fermi level results in a weak composition dependence of the electromotive force, what is advantageous from the application point of view. The lithium chemical diffusion coefficient, which determines the current density is a function of the mobility of lithium ions and electrons in the cathode materials. In the layered and skeleton structures (Fig.1), paths of rapid diffusion exist and they ensure sufficiently high mobility of

lithium ions, which does not limit the efficiency of the intercalation process. However, the localization of electronic states at the Fermi level, often observed in transition metal compounds, leads to a kinetic limitation of the intercalation process.

The first lithium battery technology i.e. $Li/Li^+/Li_xTiS_2$ cell technology was rapidly withdrawn from the market in the beginning of 70-ties of the XX-th century due to formation of lithium dendrites which short-circuit the cell. Twenty years later, in 1991, a new generation of lithium batteries, i.e. Li-ion batteries ($Li_xC_6/Li^+/Li_{1-x}CoO_2$), was commercialized by Sony Cor. The metallic lithium anode was replaced with graphite, which has the ability to reversibly intercalate lithium and has a reasonably low potential versus lithium. Charging and discharging is related to a reversible „pumping" of lithium ions from one electrode to another (subsequent, reversible intercalation and deintercalation processes). Fig.2 presents the working mechanism of Li-ion batteries.

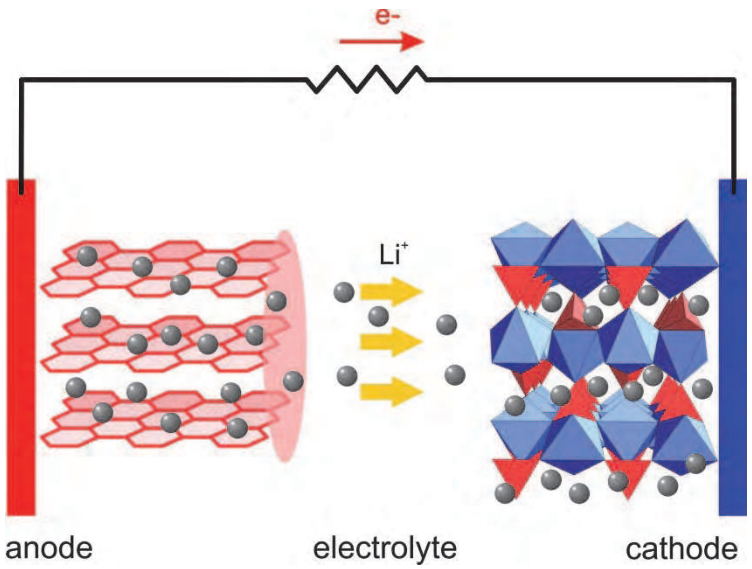

Fig. 2. Working mechanism of Li-ion batteries.

The effectiveness of the intercalation process in $Li_xC_6/Li^+/Li_{1-x}M_aX_b$ type cell, which at the graphite anode can be written as:

$$C_6 + xLi^+ + xe^- \leftrightarrow Li_xC_6 \tag{2}$$

and analogously at the cathode

$$Li_1M_aX_b \leftrightarrow Li_{1-x}M_aX_b + xLi^+ + xe^- \tag{3}$$

is determined by ionic-electronic transport properties of both electrode materials, number of sites available for lithium ions Li^+ and density of available electronic states around the Fermi level in both electrode materials. Li-ion batteries $Li_xC_6/Li^+/Li_{1-x}M_aX_b$ principle parameter, i.e. energy density – per unit mass or volume, dependent on the cell electromotive force and its capacity, is defined by electronic and crystallographic structure of both electrode materials in relation to lithium intercalation reaction. Current density of the cell depends on

ionic-electronic transport properties in both electrode materials (ambipolar diffusion). Consequently, the cell voltage, capacity, energy density and current density are defined by properties of the cathode and anode materials. The number of charge and discharge cycles and cell lifetime are significantly conditioned by processes taking place on electrode material/electrolyte interfaces. Cell safety depends on thermal and chemical stabilities of electrode materials and electrolyte. It has been shown (J. Molenda, 1997), that graphite anode does not limit Li-ion batteries operational parameters such as current density or voltage. Favourable structure properties of graphite (layered structure) and its high electrical conductivity together with delocalisation of electronic states at the Fermi level ensure a high efficiency of ionic-electronic processes in the graphite electrode. **Therefore the only way for substantial improvement of Li-batteries parameters is to improve and upgrade the cathode materials.**

Presently in the Li-ion batteries technology, beside $LiCoO_2$, there are also used as cathode materials $LiCo_{1-y}Ni_yO_2$ and $LiMn_2O_4$. However these cathode materials exhibit some practical faults. In case of $LiCoO_2$ only half of its theoretical capacity can be used. This is due to reversible intercalation/deintercalation process only within Li_1CoO_2 – $Li_{0.5}CoO_2$ range, what yields this low reversible capacity of 130 mAh g^{-1} (J. Molenda & Stokłosa, 1989). Moreover the $LiCoO_2$ is not environmental friendly and expensive. $LiNiO_2$ reveals higher reversible capacity (190 mAh g^{-1}) than $LiCoO_2$, however there are some basic difficulties in obtaining ordered structure of $LiNiO_2$ due to strong cation mixing (Li- Ni) effect in this compound, what substantially worsens its transport and electrochemical properties (J. Molenda et al., 2002). Moreover at high deintercalation degree an exothermic reaction with liquid organic electrolyte takes place. Manganese spinel $LiMn_2O_4$ exhibits phase transition at room temperature and limited stability, what decrease cyclability of the battery (J. Molenda et al., 2000; J. Molenda et al., 2004).

3. Cathode materials based on iron oxides

A cathode material for Li-ion technology based on iron oxides was always a desired object. The interest in iron compounds arises from the fact that iron is cheap, abundant in the earth crust and friendlier for the environment than cobalt, nickel or manganese. Unfortunately the first taken-intoconsideration iron-containing, layered compound $LiFeO_2$, isostructural with $LiCoO_2$ and $LiNiO_2$, is found to be metastable. Generally, stability of ABO_2 oxides with the layered structures of α-$NaFeO_2$ (R3m) type can be estimated from Pauling's rule, according to which the r_B/r_A ratio should be less than 0.86. In the case of $LiCoO_2$ and $LiNiO_2$, this ratio is 0.77 and 0.78, respectively. For $LiFeO_2$ $r{Fe^{3+}}/r{Li^+}$ = 0.88, and the structure is unstable. Another important reason, which excludes $LiFeO_2$ from the application in batteries, is disadvantageous position of redox potentials of iron in relation to those of lithium (Fig.3).

The Fe^{3+}/Fe^{4+} potential is too distant from that of Li/Li^+ and located beyond the electrochemical window of the electrolyte, which cannot guarantee the neutrality of the electrolyte versus the cathode. On the other hand, the Fe^{3+}/Fe^{2+} potential is too close to that of Li/Li^+, which results in a too low voltage of the cell. Such behavior is related to the high spin configuration of Fe^{3+} and strong interactions between the *d* electrons. The problems of structural instability and unfavorable position of redox potentials of iron versus lithium can be overcome by using new series of iron compounds, e.g. $LiFeXO_4$, as proposed by Goodenough (Goodenough, 1998) with large polyanions $(XO_4)^{y-}$ (X =S, P, As, Mo, W; y = 2 or 3) that might stabilize the structure. The presence of such $(XO_4)^{y-}$polyanions with a strong covalent bond X–O stabilizes the anti-bonding state of Fe^{3+}/Fe^{2+}. The Fe–O bond becomes

less covalent due to the induction effect in the Fe–O–X system, which raises the electrode potential in $LiFePO_4$ (Fig. 3).

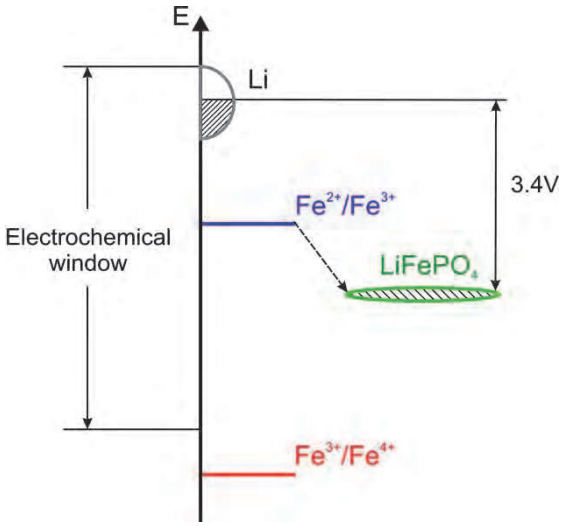

Fig. 3. Energy diagram showing the Fe^{3+}/Fe^{4+} and Fe^{2+}/Fe^{3+} potentials in the cathode materials based on iron in octahedral coordination.

4. Phospho-olivine $LiFePO_4$

The olivine structured $LiFePO_4$ belongs to a family of super ionic conductors called NaSICON, known as fast ionic conductors and used as solid electrolytes in electrochemical cells. In $LiFePO_4$, the hexagonal close-packed lattice of oxygen has one dimensional channels which act as potential fast diffusion paths for the lithium ions (Fig.4).
However, due to the specific crystal structure (FeO_6 octahedra linked via corners lead to a significant, over 4Å, Fe-Fe distance, while the M-M distance for conductive oxides is below 3Å) phospho-olivine is practically an electronic insulator. Its electrical conductivity at room temperature equals to 10^{-10}S $cm^{-1}$is extremely low as for a cathode material (Fig.5).
Low electrical conductivity is a reason for which the observed $LiFePO_4$ delithiation is not really a diffusional deintercalation process described by the following equation:

$$LiFePO_4 - xLi^+ - xe^- \leftrightarrow Li_{1-x}FePO_4 \quad (4)$$

that yields a homogeneous material with varying lithium content. Literature reports (Yang et al., 2002) and our own studies indicate that lithium extraction from $LiFePO_4$ in the charge cycle consists of decomposition of the cathode material into two phases of which one contains lithium and the other is lithium-free:

$$LiFePO_4 - xLi^+ - xe^- = xFePO_4 + (1 - x)LiFePO_4 \quad (5)$$

and a similar reverse reaction (discharging cycle):

$$FePO_4 + xLi^+ + xe^- = xLiFePO_4 + (1 - x)FePO_4 \quad (6)$$

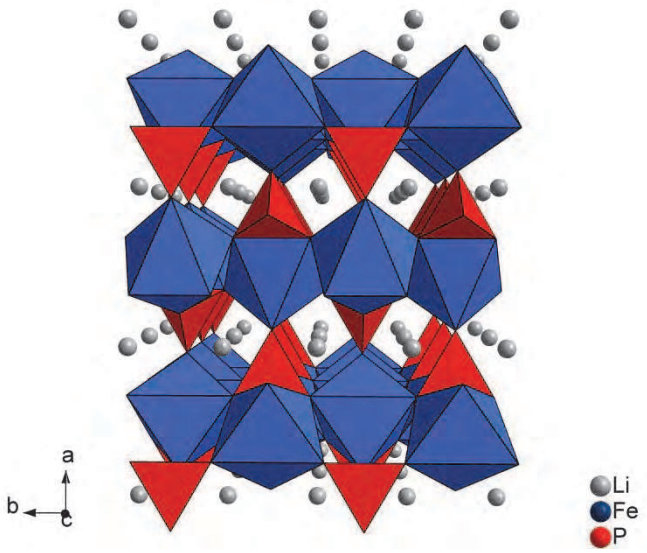

Fig. 4. Structure of $LiFePO_4$.

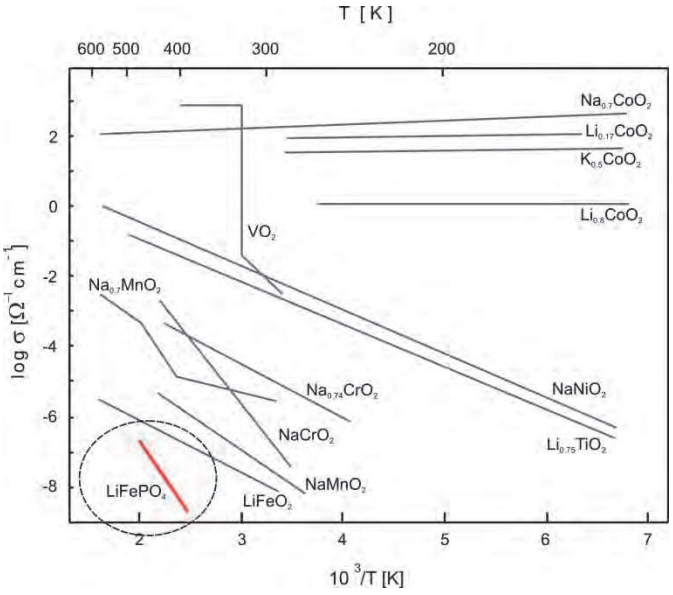

Fig. 5. Temperature dependence of electrical conductivity for different cathode materials in comparison to $LiFePO_4$.

Observed high reversibility of the charge/discharge processes is related to vast similarity of the $LiFePO_4$ and $FePO_4$ structures (the same space group and volume difference of only 6.81%). The described behavior of the cathode material is not at all beneficial – only the

grain surfaces of the cathode are effectively used and current density of the cell is low. The reason for the reactions (5) and (6) to occur is low electronic conductivity.
On the other hand, $LiFePO_4$ shows some important advantages: the highest theoretical capacity of all known cathode materials (170mAh g^{-1}), the highest thermal stability, which guarantees safety of use and stable capacity after numerous work cycles. Therefore the most challenging issue in the search for a cathode material based on phospho-olivine is to get a mixed ionic–electronic conductivity, which should activate the diffusional mechanism of deintercalation/ intercalation process (i.e. proceed according to reaction (4)).
Much hope for commercial Li-ion batteries was associated with Chiang's revolutionary report on phospho-olivine doping (Chung et al., 2002), indicating a possibility of electrical conductivity increase by a factor of 10^7. However, examination of doped phospho-olivine surfaces by J. Molenda et al. (Marzec et al., 2006; Ojczyk et al. 2007) and the results published by Nazar (Herle et al., 2004) have proved that the high values of conductivity of doped phospho-olivine are not due to bulk metallic properties but due to the formation of metallic iron phosphides on the surface of phospho-olivine grains, which are the effect of partial reduction of $LiFePO_4$ to Fe_2P during the synthesis (Fig. 6). Formation of Fe_2P showing metallic type conductivity on the surface of the $LiFePO_4$ grains in the course of phospho-olivine synthesis, give rise to an effective technology for producing composite $LiFePO_4$–Fe_2P cathode materials, exhibiting remarkably improved properties.

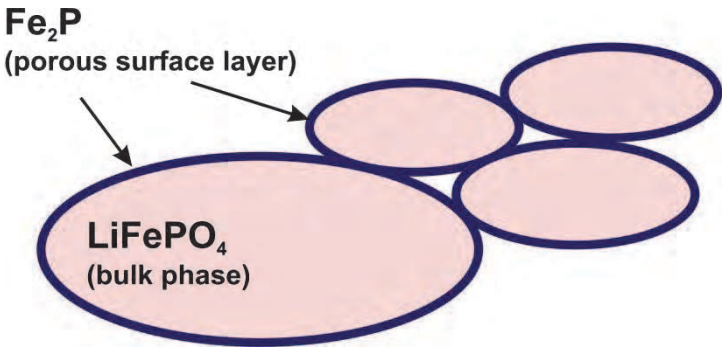

Fig. 6. Composite $LiFePO_4$–Fe_2P cathode material.

5. Preparation of a composite phase $LiFePO_4$–Fe_2P

For a successful preparation of the Fe_2P films on the phospho-olivine grains, the presence of a highly reducing agent is required. Such a reducing agent should be formed during the synthesis process, being an intermediate product of the reaction between $Fe_2C_2O_4$ xH_2O, $NH_4H_2PO_4$ and Li_2CO_3 (Fe, $Fe_x(CO)_y$, C, Co and NH_3). The analysis of chemical properties of the particular substrates indicates that the reducing agent can be possibly formed as a product of a $FeC_2O_4 \cdot 2H_2O$ thermal decomposition reaction. However, the results of a thermal analysis (MS-TGA/DTG) carried over the thermal decomposition of $FeC_2O_4 \cdot 2H_2O$ has shown that the mechanism of the decomposition reaction strongly depends on the reaction environment. Our investigations demonstrated that the maximum amount of the reducing agent, namely fine dispersed iron nanoparticles, was obtained during the decomposition carried in a dry argon flow. This condition seems to be crucial, since the

presence of steam in the reaction environment causes a secondary oxidation of iron and, consequently, a disappearance of the reducing agent, according to the reaction:

$$3Fe + 4H_2O = Fe_3O_4 + 4H_2\uparrow \quad (7)$$

A formation of the lower oxides is also possible in case of the steam deficiency (playing the role of the oxidizing agent). A uniform dispersion of the reducing agent is also required for the creation of Fe_2P thin layer on the $LiFePO_4$ phospho-olivine surface. On the basis of the synthesis tests previously performed, we found that the best results were achieved for the reaction mixtures milled in a ball mill. The additional DSC measurements demonstrated that milling the reaction mixture affects the water distribution in the system (Ojczyk et al., 2007). Iron nanoparticles as a reducing agent is highly unstable in the presence of even trace amounts of oxygen. Still, when it is rapidly exposed to the environment with a high concentration of oxygen (like air), it may undergo a passivation reaction (a surface oxidation and the formation of a protective, gas-tight oxide layer). In our case it can be assumed that the oxide layer, resulting from the passivation, prevented the oxidation of the reducing agent with oxygen from air at the intermediate stage of the synthesis, i.e. milling of the mixture after the calcinations at 350°C (Ojczyk et al., 2007).
The formation of iron phosphide Fe_2P resulting from the reduction of phosphate radicals with iron nanoparticles occurs only at higher temperatures (above 600°C). Below this temperature iron can be oxidized with oxygen residues. Consequently, the exposure time of the reaction mixture at low temperatures should be as short as possible, therefore high rates of the furnace heating up to the optimum reaction temperature are essential. The results of a thermal analysis for the reaction mixtures yielded a temperature of 800°C for 10 h as the optimum synthesis conditions (Ojczyk et al., 2007).
On the basis of the obtained results of thermal analysis and synthetic route trials, it can be concluded that a thin layer of Fe_2P can be formed only when the appropriate conditions of the synthesis process are satisfied:

- The products of the reaction (H_2O) can be carried away properly from the reactor at the volume flow rate (F_v) of the carrying gas (Ar = 99.999%, O_2<0.0005%) being at least: $F_v = 20V_{react}/t$ for 1 g of the reagents batch

where: F_v — volume flow rate [cm^3 min^{-1}]; V_{react} — the pipe flow reactor volume [cm^3]; t — time =60 minutes, both at the initial stage of the decomposition (350°C) and the main high-temperature reaction (800°C),

- Linear rate of carrying gas over the reagents should be at least 0.5 cm s^{-1}; this would prevent secondary reactions (iron oxidation)
- Milling the substrates in a ball mill prior to the reaction ensures an appropriate dispersion of the substrates
- A high heating rate (β= 10°min^{-1}), ensuring the maximum concentration of the reductive agent at the optimal temperature of the re action (800°C).

6. Carbon composite electrode materials

The high performance lithium ion batteries need electrode (cathode and anode) materials showing high ionic and electronic conductivities as well as high chemical stability, as it was mentioned above. Currently, the standard composite cathodes used in Li-ion cells are prepared as physical mixture of powders (active material, carbon and binder) (Tarascon &

Armand, 2001). Higher performances of cathode as well as anode materials may be achieved by lowering the size of active material grains. Nanosized grains reveal better electrochemical properties and also lower chemical stability towards electrolyte (Armand &Tarascon, 2008). The latest may provide dangerous and uncontrolled self ignition of a cells. Coating of active material by conductive carbon layer (CCL) increase the chemical stability and safety of the composite cathode (M. Molenda et al., 2008). There are many reports on the improvement of electrochemical performance of electrode materials for lithium-ion batteries using carbon coatings (Armand &Tarascon, 2008; Cushing & Goodenough, 2002; Kim et al., 2008; Lin et al., 2008; Kim, et al., 2008; Fey et al., 2008; Choi et al., 2008; Guo et al., 2009; Hassoun et al., 2008). The compounds reported for the coating formation include carboxylic acids (Lin et al., 2008), poly-alcohols (Guo et al., 2009), resins (Cushing & Goodenough, 2002; He et al., 2007) and sugars (Kim et al., 2008). To form the carbon coating, the compounds were deposited on the electrode material grains and pyrolysed, from which carbon layers resulted. However, the morphology of these layers was not discussed in detail. Characteristic of the carbon coatings deposited on electrodes is that they can react with the electrolyte thereby giving rise to the formation SEI or of passive insulating layers. The carbon coatings formed as carbon matrixes are applied in silica, tin or antimony based high capacity anode composites (Ng et al., 2007; He et al., 2007; Trifonova et al., 2008; Li & Li, 2008; Hassoun et al., 2008). In such the composites the carbon layers act as conducting and stress buffering agent compensating a volume changes during lithium insertion-deinsertion from active material, avoiding lost of electrical contact in the composite. However, high capacity electrodes requires a nano-sized grains of active materials which reveal high chemical reactivity thus it makes difficult the composites preparation. A novel method of preparation of conductive carbon layers with controlled morphology on fine particle powders, based on direct polymer deposition, has been developed by M. Molenda et al. (M. Molenda et al., 2007, 2008, 2010).

7. Preparation and properties of carbon coatings

A model of carbon coatings or carbon matrixes formation process are presented on Figs. 7. In this process prepared model $C/\alpha{-}Al_2O_3$ composites to revealed the possibility of control of the CCL morphology and its electrical properties. Two ways of the composite precursors formation can be applied. In the first (Fig. 7A), the free-radical precipitation polymerization of freshly distilled acrylonitrile (AN) was performed in the presence of $\alpha{-}Al_2O_3$ grains (POCh, Poland, 99.99 %, S_{BET} = 24 m^2g^{-1}), according to procedure described by M. Molenda et al. (M. Molenda et al., 2007). In brief, $\alpha{-}Al_2O_3$ grains were suspended in water solution of AN (7 wt%) and the polymerization was initiated by 2,2'-azobis(isobutyramidine hydrochloride) (Aldrich), upon which the obtained $PAN/\alpha{-}Al_2O_3$ samples were washed, filtered and dried in the vacuum at 50°C. In the second way (Fig. 7B), the $\alpha{-}Al_2O_3$ grains were impregnated with polymers composition in water solutions. The polymers used, were poly-N-vinylformamide (PNVF) obtained by radical-free polymerization from N-vinylformamide (Aldrich) (M. Molenda et al., 2008) and pyromellitic acid (PMA) modified (5-10 wt%) PNVF (called MPNVF) (M. Molenda et al., 2010). To achieve the impregnation, $\alpha{-}Al_2O_3$ grains were suspended in the solutions of respective polymers in water (8-15 wt%).

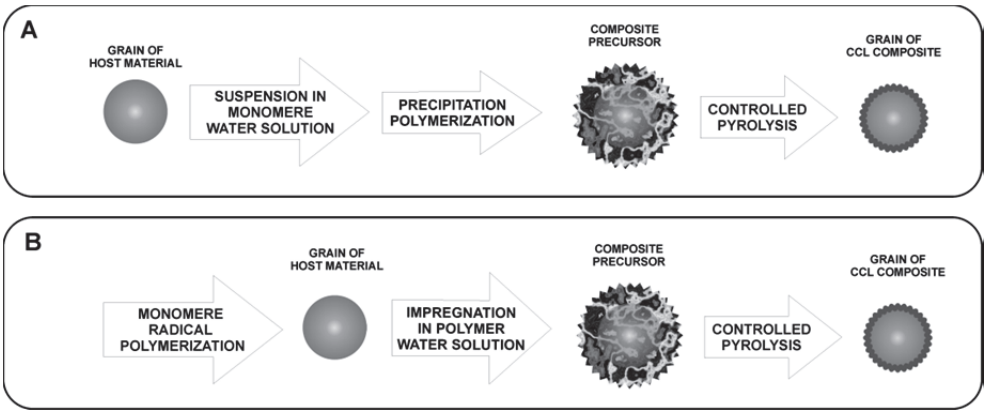

Fig. 7. Process for the preparation of conductive carbon layers (CCL) on powdered support.

The suspensions were stirred continuously until the solvent evaporated and the viscosity of the solutions became high enough to avoid sedimentation. Then the samples were dried in an air drier at 90°C overnight. To obtain C/α–Al_2O_3 composites, following the preparation, the polymer/α–Al_2O_3 composite precursors were pyrolysed in a tube furnace under the flow of 99.999 % argon (5 dm^3/h) at 550° and 600°C for 24h. The C/α–Al_2O_3 composites were deep black with foamed slag-like structure or lustrous and glassy like graphite (for PMA modified PNVF carbon precursor).

Electrical properties of the model C/α–Al_2O_3 composites, presented in Fig. 8, reveal increase of the electrical conductivity with an increase in carbon loading. For the model support, the minimal carbon loading for electrical conductivity through CCL (continuous path) is above 12 wt% of C. However, below this limit a conduction percolation path formation is observed. By a contrast, the activation energy of electrical conductivity remained nearly constant, suggesting a preservation of the conductivity mechanism through the CCL. The best electrical properties, i.e. the highest conductivity and the lowest activation energy, were revealed by the model composite based on the MPNVF precursor. This behavior was supported by the results of the Raman spectroscopy (RS) (Fig. 9).

The correlation between degree of carbon materials graphitization, characterized by intensity ratio of D/G bands, were found. The D band (defect mode; at about 1350 cm^{-1}) corresponds to sp^3 diamond-like carbon structures while the G band (about 1600 cm^{-1}) corresponds to sp^2 graphitic structures (Ferrari & Robertson, 2000; Fauteux et al., 2004; Osswald et al. 2005; Pantea et al., 2001). The graphitization degree (decrease in the D/G ratio) significantly increased after PMA modification of PNVF polymer, what may suggest formation of the highest amounts of the graphene domains in CCL. Also downshift and width decrease of the G peak of the carbonized MPNVF precursor suggest 2D ordering (1st phase of graphitization) (Fauteux et al., 2004). The improvement of the polymer carbonization upon CCL formation after PMA modification may results from the fact that planar structure of pyromellitic acid molecules serve as a nucleus of the graphene domains, and compete with the formation of the disordered structures.

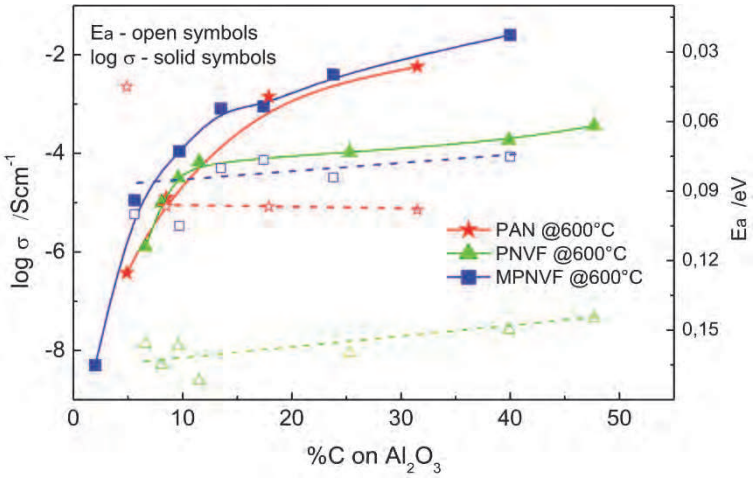

Fig. 8. Electrical properties of the model C/α−Al_2O_3 composites.

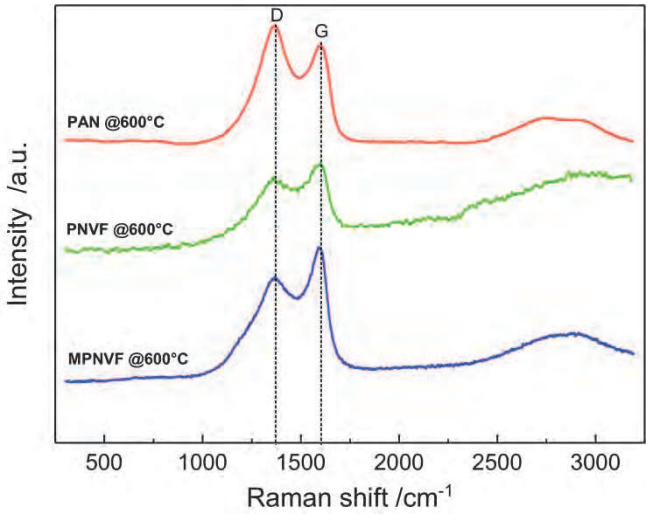

Fig. 9. Raman spectra of pyrolytic carbon coatings obtained from different polymer precursors.

In terms of SEI formation, a specific surface area of the CCL coating should be controlled as well as its pores structure. The resulting specific surface area of the composite depends on polymer precursor used (Fig. 10) and increases linearly with carbon loading up to 25-30 wt%.

This suggests that the initial porous structure of the CCLs is preserved regardless of the carbon content. The PMA modification of polymer precursor results in reducing of specific surface area of formed CCL, probably with locally arranged graphene domains what limits the formation of disordered carbon.

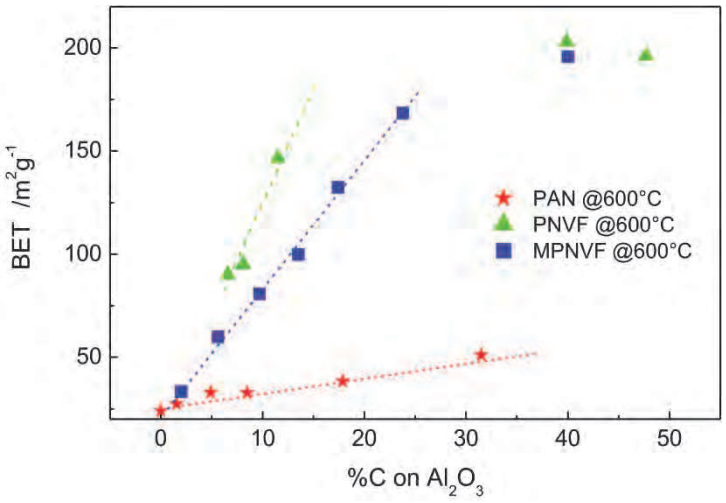

Fig. 10. Specific surface area of the composites as function of carbon loading.

The pores structure and morphology of the CCL in the model C/α–Al_2O_3 composites evaluated from N_2-adsorption-desorption isotherms (Fig. 11) reveal strong dependence on starting polymer composition (carbon precursor). The observed shapes of the isotherms (Fig. 11a-11c) correspond to the mixed I and IV types of isotherms (according to IUPAC nomenclature). Such shapes indicate the presence of micro- and mesopores within the CCLs. The hysteresis loops of the H4 type (IUPAC) suggest the slotted pores located within the intergranular spaces. The pore size and their distribution varies on carbon precursor used (Fig. 11d-11f) and may be controlled by optimization of polymer composition, e.g. modification of PNVF by PMA results in very uniform distribution of the mesopores with sizes within the range of 3-4.5 nm (Fig. 11f).

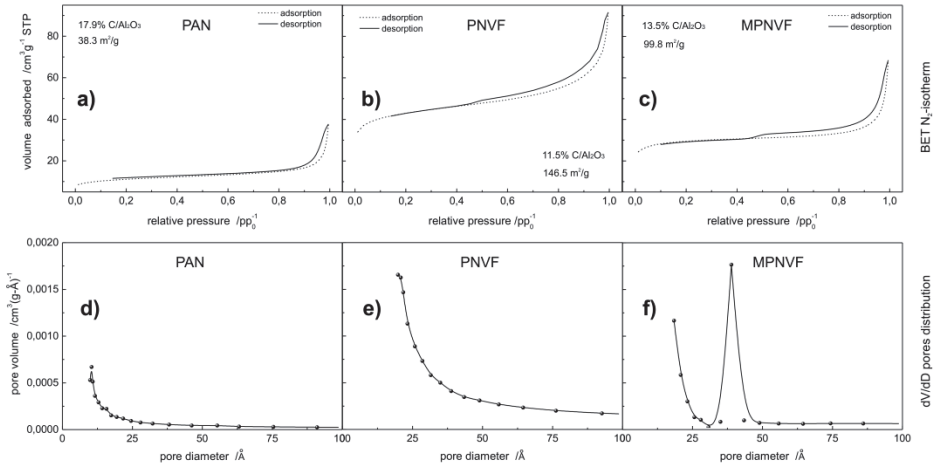

Fig. 11. BET N_2-adsorption-desorption isotherms and pore size distribution of the composites.

The morphological and electrical properties as well as observed local structure suggest the following structural model of the C/α–Al_2O_3 composites derived from the polymer precursors (Fig. 12).

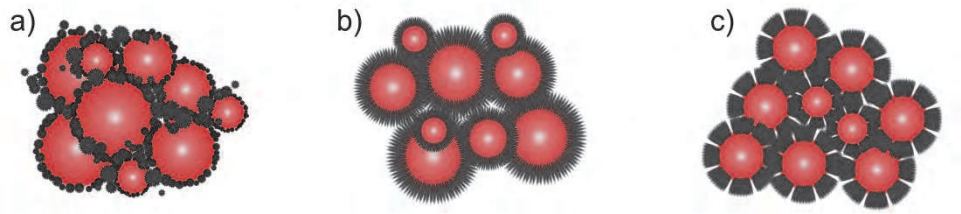

Fig. 12. Structural model of the CCL carbon coatings.

The CCL obtained from the PAN precursor (Fig. 12a) consists of tightly packed small carbon particles, while that obtained from the PNVF precursor (Fig. 12b) is built of carbon whiskers, this latter structure being reflected in a high specific surface area and a high share of the micropores in this sample. This same PNVF precursor, after modification with pyromellitic acid, strongly diminishes the specific surface area of the resulting composite, which is due to the formation of a tight, highly conductive carbon film with the defined porous structure that is dominated by mesopores with a narrow size distribution (Fig. 12c). The formed CCL coating build of amorphous carbon is thin and uniformly dispersed on the host grains what can be seen from HR-TEM picture (Fig. 13).

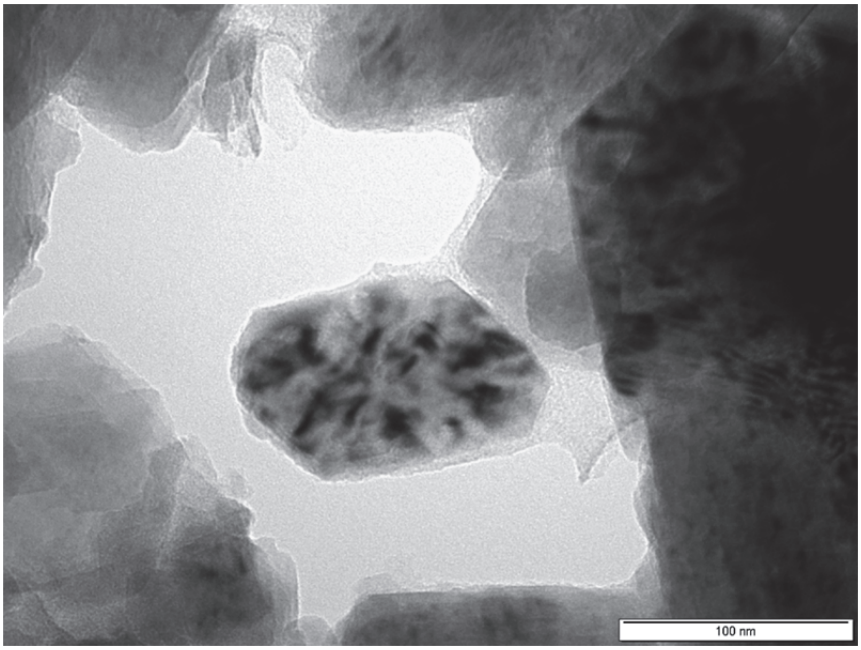

Fig. 13. HR-TEM picture of the C/α–Al_2O_3 composite.

8. Acknowledgements

This work was financially supported by EU under the grant No. UDA-POIG 01.01.02-00-108/09-01.

9. References

Chung, S.Y., Bloking, J.T. & Chiang, Y.M., Electronically conductive phospho-olivines as lithium storage electrodes. *Nature Materials*, Vol. 1, No. 2, (October 2002), pp. 123-128.

Goodenough, J.B. (1998). *General concepts*, In: Lithium Ion Batteries. Fundamentals and Performance, Wakihara, M., Yamamoto, O., pp. 1-25, Wiley-VCH, ISBN: 9783527295692, Tokyo.

Herle, P.S., Ellis, B., Coombs, N. & Nazar, L.F. , Nano-network electronic conduction in iron and nickel olivine phosphates. *Nature Materials*, Vol. 3, No. 3, (March 2004), pp. 147-152.

Marzec, J., Ojczyk, W. & Molenda, J. , Delithiation of olivine- structured $LiFe_xMn_{1-x}PO_4$ cathode materials. Mössbauer studies. *Materials Science-Poland*, Vol. 24, No. 1, (2006), pp. 69-74.

Molenda, J., Bąk, J. Effect of tungsten on the electrical and electrochemical properties of the $Li_yW_xVO_2$ cathode. *Physica Status Sololidi (a)*, Vol. 135, No. 1, (1993), pp. 263-271.

Molenda, J., Kubik, A., Transport properties and reactivity of tungsten trioxide. *Solid State Ionics*, Vol. 117, No. 1-2 (February 1999), pp. 57-64.

Molenda, J., Stokłosa, A. Electronic structure and electrochemical properties of VO_2. *Solid State Ionics*, Vol. 36, No. 1-2, (October 1989), pp. 43-52.

Molenda, J., Bąk, T. & Stokłosa, A., Influence of lithium on the electronic structure of $YBa_2Cu_3O_{7-\delta}$. *Physica C*, Vol. 207, No. 1-2 (March 1993), pp. 147-158.

Molenda, J., Świerczek, K., Molenda, M. & Marzec, J., Electronic structure and reactivity of $Li_{1-x}Mn_2O_4$ cathode. *Solid State Ionics*, Vol. 135, No. 1-4, (November 2000), pp. 53-59.

Molenda, J., Wilk P. & Marzec, J. Structural, electrical and electrochemical properties of $LiNiO_2$. *Solid State Ionics*, Vol. 146, No. 1-2, (January 2002) 73-79.

Molenda, J., Marzec, J. ,Świerczek, K., Ojczyk, W., Ziemnicki, M., Molenda, M., Drozdek, M. & Dziembaj, R. The effect of 3d substitutions in the manganese sublattice on the charge transport mechanism and electrochemical properties of manganese spinel. *Solid State Ionics*, Vol. 171, No. 3-4, (July 2004), pp. 215-227.

Molenda, J., Ojczyk, W., Świerczek, K., Zając, W., Krok, F., Dygas, J. & Liu, R.S. Diffusional mechanism of deintercalation in $LiFe_{1-y}Mn_yPO_4$ cathode material. *Solid State Ionics*, Vol. 177, No. 26-32, (October 2006), pp. 2617-2624.

Molenda, J. Correlation between electronic and electrochemical properties of carbon. *Bulletin of Polish Academy of Sciences - Chemistry*, Vol. 45, (1997) pp. 449.

Molenda, J. Electronic limitations of lithium diffusibility. From layered and spinel toward novel olivine type cathode materials. *Solid State Ionics*, Vol. 176, No. 19-22, (June 2005), pp. 1687-1694.

Ohzuku, T. *Four-volt cathodes for lithium accumulators and the Li-ion battery concept*, In: Lithium Batteries, New Materials, Development and Perspectives, Pistoia, G., pp. 239-280, Elsevier, Amsterdam.

Ojczyk, W., Marzec, J., Świerczek, K., Zając, W., Molenda, M. , Dziembaj, R. & Molenda, J. Studies of selected synthesis procedures of the conducting $LiFePO_4$-based composite cathode materials for Li-ion batteries. *Journal Power Sources*, Vol. 173, No. 2, (November 2007), pp. 700-706.

Tarascon, J.-M. & Armand, M. Issues and challenges facing rechargeable lithium batteries. *Nature*, Vol. 414, (November 2001) pp. 359-367.

Than, D., Molenda, J. & Stokłosa A. Correlation between electronic and electrochemical properties of $Li_xTi_{1+y}S_2$. *ElectrochimicaActa*, Vol.36 No. 10, (1991), pp. 1555-1560.

Whittingham, M.S. Chemistry of intercalation compounds: Metal guests in chalcogenide hosts. *Prog. Solid State Chem.*, Vol. 12, No. 1, (1978), pp. 41-99.

Yang, S., Song, Y., Zavalij, P.Y. & Whittingham, M.S., Reactivity, stability and electrochemical behavior of lithium iron phosphates. *Electrochemistry Communications*, Vol. 4, No. 3, (March 2002) pp. 239-244.

Armand, M. &Tarascon, J.-M, Building better batteries. *Nature*, Vol. 451 (February 2008) pp. 652-657.

Molenda, M., Dziembaj, R., Piwowarska, Z. & Drozdek M., Electrochemical properties of $C/LiMn_2O_{4-y}S_y$ ($0 \le y \le 0.1$) composite cathode materials. *Solid State Ionics,* Vol. 179 No. 1-6 (2008) pp. 88-92.

Cushing, B.L. & Goodenough, J.B., Influence of carbon coating on the performance of a $LiMn_{0.5}Ni_{0.5}O_2$ cathode. *Solid State Science,* Vol. 4, (2002) pp. 1487-1493.

Kim, J.K., Cheruvally, G., Ahn, J.H. & Ahn, H.J., Electrochemical properties of $LiFePO_4/C$ composite cathode material: Carbon coating by the precursor method and direct addition. *Journal of Physics and Chemistry of Solids*, Vol. 69, (2008) pp. 1257-1260.

Lin, B., Wen, Z., Han J. & Wu X., Electrochemical properties of carbon-coated $Li[Ni_{1/3}Co_{1/3}Mn_{1/3}]O_2$ cathode material for lithium-ion batteries. *Solid State Ionics*, Vol. 179, (2008) pp. 1750-1753.

Kim, J.K., Cheruvally, G. & Ahn, J.H., Electrochemical properties of $LiFePO_4/C$ synthesized by mechanical activation using sucrose as carbon source. *Journal of Solid State Electrochemistry*, Vol. 12, (2008) pp. 799-805.

Fey, G.T.K., Lu, T.L. & Wu, F.Y., Carboxylic acid-assisted solid-state synthesis of $LiFePO_4/C$ composites and their electrochemical properties as cathode materials for lithium-ion batteries. *Journal of Solid State Electrochemistry*, Vol. 12, (2008) pp. 825-833.

Choi, Y.J., Chung, Y.D., Baek, C.Y., Kim, K.W., Ahn, H.J. & Ahn, J.H., Effects of carbon coating on the electrochemical properties of sulfur cathode for lithium/sulfur cell. *Journal of Power Sources,* Vol. 184, (2008) pp. 548-552.

Guo, R., Shi, P., Cheng, X. & Du, C., Synthesis and characterization of carbon-coated $LiNi_{1/3}Co_{1/3}Mn_{1/3}O_2$ cathode material prepared by polyvinyl alcohol pyrolysis route. *Journal of Alloys Compounds*, Vol. 473, (2009) pp. 53-59.

Ng, S.H., Wang, J., Konstantinov, K., Wexler, D., Chew, S.Y., Guo, Z.P. & Liu, H.K., Spray-pyrolyzed silicon/disordered carbon nanocomposites for lithium-ion battery anodes. *Journal Power Sources*, Vol. 174, (2007) pp. 823-827.

He, X., Pu, W., Wang, L., Ren, J., Jiang, C. & Wan, C., Synthesis of spherical nano tin encapsulated pyrolyticpolyacrylonitrile composite anode material for Li–ion batteries. *Solid State Ionics,* Vol. 178, (2007) pp. 833-836.

Trifonova, A., Stankulov, T. & Winter, M., Study of metal-supported carbon matrix as a high-capacity anode for Li-ion battery. *Ionics*, Vol. 14, (2008) pp. 421-425.

Li Y. & Li J., Carbon-Coated Macroporous $Sn_2P_2O_7$ as Anode Materials for Li-Ion Battery. *Journal of Physical Chemistry C*, Vol. 112, (2008) pp. 14216-14219.

Hassoun, J., Derrien, G., Panero, S. & Scrosati, B., The role of the morphology in the response of Sb–C nanocomposite electrodes in lithium cells. *Journal of Power Sources*, Vol. 183, (2008) pp. 339-343.

Molenda, M., Dziembaj, R., Piwowarska, Z. & Drozdek, M., A new method of coating powdered supports with conductive carbon films. *Journal of Thermal Analysis and Calorimetry,* Vol. 88, (2007) pp. 503–506.

Molenda, M., Dziembaj, R., Podstawka, E., Proniewicz, L.M. & Piwowarska, Z., An attempt to improve electrical conductivity of the pyrolysed carbon-$LiMn_2O_{4-y}S_y$ ($0<y<0.5$) composites, *Journal of Power Sources,* Vol. 174, (2007) pp. 613-618.

Molenda, M., Dziembaj, R., Drozdek, M., Podstawka, E. & Proniewicz, L.M., Direct preparation of conductive carbon layer (CCL) on alumina as a model system for direct preparation of carbon coated particles of the composite Li-ion electrodes. *Solid State Ionics,* Vol. 179, (2008) pp. 197–201.

Molenda, M., Dziembaj, R., Kochanowski, A., Bortel, E., Drozdek, M. & Piwowarska, Z., Process for the preparation of conductive carbon layers on powdered supports, *Patent Application*, WO 2010/021557 A2 (2010).

Ferrari, A.S. & Robertson J., Interpretation of Raman spectra of disordered and amorphous carbon. *Physical Review B*, Vol. 61, (2000) pp. 14095-14107.

Fauteux, C., Longtin, R., Pegna, J. & Boman, M., Raman characterization of laser grown carbon microfibers as a function of experimental parameters. *Thin Solid Films*, Vol. 453-454, (2004) pp. 606-610.

Osswald, S., Flahaut, E., Ye, H. & Gogotsi, Y., Elimination of D-band in Raman spectra of double-wall carbon nanotubes by oxidation. *Chemical Physics Letters*, Vol. 402, No. 4-6, (2005) pp. 422-427.

Pantea, D., Darmstadt, H., Kaliaguine, S., Summchen, L., & Roy, C., Electrical conductivity of thermal carbon blacks - Influence of surface chemistry. *Carbon*, Vol. 39, No. 8, (2001) pp. 1147-1158.

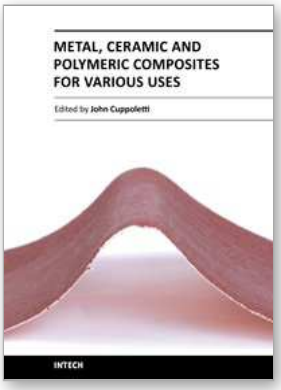

Metal, Ceramic and Polymeric Composites for Various Uses

Edited by Dr. John Cuppoletti

ISBN 978-953-307-353-8
Hard cover, 684 pages
Publisher InTech
Published online 20, July, 2011
Published in print edition July, 2011

Composite materials, often shortened to composites, are engineered or naturally occurring materials made from two or more constituent materials with significantly different physical or chemical properties which remain separate and distinct at the macroscopic or microscopic scale within the finished structure. The aim of this book is to provide comprehensive reference and text on composite materials and structures. This book will cover aspects of design, production, manufacturing, exploitation and maintenance of composite materials. The scope of the book covers scientific, technological and practical concepts concerning research, development and realization of composites.

How to reference

In order to correctly reference this scholarly work, feel free to copy and paste the following:

Janina Molenda and Marcin Molenda (2011). Composite Cathode Material for Li-Ion Batteries Based on LiFePO4 System., Metal, Ceramic and Polymeric Composites for Various Uses, Dr. John Cuppoletti (Ed.), ISBN: 978-953-307-353-8, InTech, Available from: http://www.intechopen.com/books/metal-ceramic-and-polymeric-composites-for-various-uses/composite-cathode-material-for-li-ion-batteries-based-on-lifepo4-system-

INTECH
open science | open minds

InTech Europe
University Campus STeP Ri
Slavka Krautzeka 83/A
51000 Rijeka, Croatia
Phone: +385 (51) 770 447
Fax: +385 (51) 686 166
www.intechopen.com

InTech China
Unit 405, Office Block, Hotel Equatorial Shanghai
No.65, Yan An Road (West), Shanghai, 200040, China
中国上海市延安西路65号上海国际贵都大饭店办公楼405单元
Phone: +86-21-62489820
Fax: +86-21-62489821